Semiconductor Science and Technology

PAPER

Characterization of MOCVD regrown *p*-GaN and the interface properties for vertical GaN power devices

To cite this article: Kai Fu *et al* 2021 *Semicond. Sci. Technol.* **36** 014005

IOP Publishing Semiconductor Science and Technology
Semicond. Sci. Technol. **36** (2020) 014005 (6pp) https://doi.org/10.1088/1361-6641/abc7d1

Characterization of MOCVD regrown *p*-GaN and the interface properties for vertical GaN power devices

Kai Fu[1], Xin Qi[1], Houqiang Fu[2], Po-Yi Su[3], Hanxiao Liu[3], Tsung-Han Yang[1], Chen Yang[1], Jossue Montes[1], Jingan Zhou[1], Fernando A Ponce[3] and Yuji Zhao[1]

[1] School of Electrical, Computer and Energy Engineering, Arizona State University, Tempe, AZ 85287, United States of America
[2] Department of Electrical and Computer Engineering, Iowa State University, Ames, IA 50011, United States of America
[3] Department of Physics, Arizona State University, Tempe, AZ 85287, United States of America

E-mail: kaifu@asu.edu and yuji.zhao@asu.edu

Received 29 August 2020, revised 1 November 2020
Accepted for publication 5 November 2020
Published 25 November 2020

Abstract

p-type gallium nitride (GaN) layers were regrown on etched surfaces on free-standing GaN substrates by metalorganic chemical vapor deposition with different growth rates by adjusting trimethylgallium flow rates. The roughness of the samples increases almost linearly with the growth rate, with an increase rate of 0.6 nm (μm h^{-1}) $^{-1}$. The screw dislocation density of the samples increases significantly when the growth rate is higher than 0.5 μm h^{-1}. When the magnesium (Mg) doping concentration is higher than 7.0×10^{19} cm^{-3}, transmission electron microscopy images clearly show the regrowth interfaces, and Mg precipitate occur in high-doping *p*-GaN layers. Under the same bis(cyclopentadienyl)magnesium (Cp_2Mg) flow rate, the Mg doping concentration decreases with the growth rate. The samples with different growth rates show different electroluminescence spectra. The emission peak at 2.8 eV is due to the transition from the deep donor level to the Mg acceptor level. And the intensity of this peak drops with increasing growth rate due to reduction of Mg acceptors. Transitions related to defect levels appears with increasing growth rate due to an increased screw dislocation density.

Keywords: gallium nitride, regrow, interface, *p*-GaN, growth rate

(Some figures may appear in colour only in the online journal)

1. Introduction

Gallium nitride (GaN) has been widely researched in recent years for optoelectronics, photonics and electronics. GaN is especially considered as a promising material for power electronics due to its wide bandgap, large breakdown electric field and high operation temperature [1–3]. In order to achieve high performance and flexible design of GaN power devices, selective-area doping is indispensable. Ion implantation, dopant diffusion, and epitaxial growth (or regrowth) are the most common approaches to realize the selective-area doping. However, it has been reported that GaN was not very resistant to ion beam disordering, and the problem became more severe at higher doses [4]. Besides, high density of dislocations in GaN can strongly affect the effective diffusion penetration depth, and the surface dissociation becomes worse during high-temperature annealing [5]. Currently, regrowth is still one of the most effective and feasible approaches to obtain well-controlled selective-area doping for GaN devices.

Regrowth has been applied to many device structures for various purposes. A selectively regrown emitter has been reported for use in GaN bipolar junction transistors (BJT) [6]. Recessed-gate structures for the metal-semiconductor field-effect transistor and AlGaN/GaN heterostructure field effect transistors have been realized by regrowth [7–9]. Regrown ohmic contact layers for source and drain electrodes have

shown to be effective in reducing specific contact resistance [10–13]. Regrown AlGaN/GaN layers have been successfully applied to vertical GaN power transistors with high performance [14, 15]. Interfaces created by regrown *p*-GaN have been reported to show threshold switching and memory behaviors with high temperature stability [16]. Regrown *p*-GaN for vertical GaN *p-i-n* diodes has been reported to achieve high breakdown voltages [17, 18].

The regrowth of *p*-GaN is an extremely important part for achieving high-performance and flexible design of GaN power devices, such as junction barrier Schottky diodes, floating field rings, junction termination extension, field effect transistors and BJT. To achieve selective-area doping by regrowth, an etch-then-regrow process is usually needed. The regrowth process can introduce impurities such as carbon (C), oxygen (O), and silicon (Si), which are extremely undesired and will degrade the performance of GaN devices [19]. Compared with C and O, the residual Si is more problematic for regrowth since it is very difficult to be removed. And it is still unclear where the Si comes from although many efforts have been made to reduce the contaminants [18, 20–24]. Besides, the dry etching process can introduce etching damage at the regrowth interface. The existence of the contaminants at the interface may be unproblematic or even beneficial for the regrown n^+-GaN as ohmic contacts because Si atoms serve as donors used for *n*-type doping. However, the residual Si is a big problem for the regrowth of *p*-GaN due to compensation.

Many fundamental problems in *p*-GaN regrowth remain to be solved; however, there are few reports so far on the topic. Although the effects of growth rate on as-grown *p*-GaN material properties have been investigated very well, few reports have been found on the regrown *p*-GaN with different growth rates, especially considering the regrowth interface. In this work, *p*-GaN layers with different growth rates were regrown on GaN free-standing substrates by metalorganic chemical vapor deposition (MOCVD). The effects of the growth rate on surface roughness, crystal quality, magnesium (Mg) doping concentration, interface properties, electroluminescence (EL) and defect levels have been investigated.

2. Experimental details

The samples were grown by MOCVD on c-plane GaN free-standing substrates with Si doping concentration of ~10^{18} cm^{-3}. Three GaN substrates were first loaded into the chamber, and 1 μm thick n-GaN was grown as the buffer layer followed by 2 μm thick unintentionally doped (UID) GaN as the drift layer. To investigate the effects of dry etching on the properties of regrown *p*-GaN, chlorine-based inductively coupled plasma (ICP) etching was used to etch away 500 nm of the GaN drift layer, creating an etched surface for the etch-then-regrow process. The RF and ICP powers of the ICP etching were 70 W and 400 W, respectively. The chamber pressure was 5 mTorr. The samples were cleaned using acetone, isopropyl alcohol and de-ionized water and then re-loaded into the chamber to regrow a 500 nm thick *p*-GaN layer with different growth rates that were controlled by adjusting the trimethylgallium flow rate under the same bis(cyclopentadienyl)magnesium (Cp_2Mg) flow rate of 0.15 μmol min^{-1}. The samples are denoted as sample A, sample B, and sample C for growth rates of 0.5 μm h^{-1}, 1.0 μm h^{-1}, and 2.0 μm h^{-1}, respectively. Rapid thermal annealing at 700 °C for 20 min in N_2 ambient was used to activate Mg acceptors in the *p*-GaN layers. Figure 1 shows the structures and etch-then-regrow process for the samples.

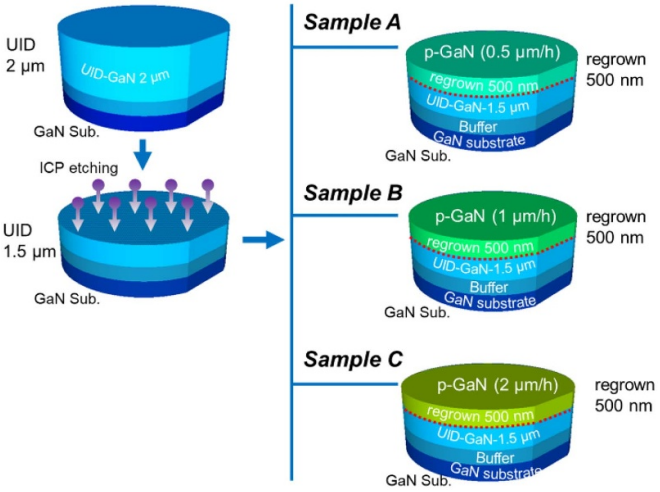

Figure 1. Schematic structures and etch-then-regrow process of GaN *p–n* junctions with different growth rates on GaN substrates grown by MOCVD.

3. Results and discussion

Before the regrowth of *p*-GaN, the root-mean-square (RMS) roughness of the UID-GaN layers for all the samples before and after the ICP etching was about 0.16 nm and 0.20 nm, respectively, measured by atomic force microscope (AFM). The roughness before/after the ICP etching was very small compared with reported results [25–27]. Figure 2 shows the surface roughness of the samples after the regrowth. The RMS roughness of sample A, sample B, and sample C is 0.66 nm, 1.02 nm, and 1.58 nm, respectively. The roughness of the samples increased after the regrowth of *p*-GaN compared with the roughness after etching. Meanwhile, the roughness of the samples increases almost linearly with the growth rate. The increase rate is around 0.6 nm $(\mu m\ h^{-1})^{-1}$. This indicates that high growth rate can degrade the surface morphology of regrown *p*-GaN layers. It is believed that with the increase of growth rate, there is less time for atoms to migrate laterally on the surface to form a good layer-by-layer growth especially when there is a small miscut angle for the GaN substrate, thereby leading to a rougher surface. The high growth rate can also exacerbate the formation of steps which thereby exacerbate the formation of screw dislocation which agrees well with the following results.

The crystal quality of the samples was characterized using x-ray diffraction (XRD) rocking curves (RCs) for symmetric (002) and asymmetric (102) planes, as shown in figures 3(a)

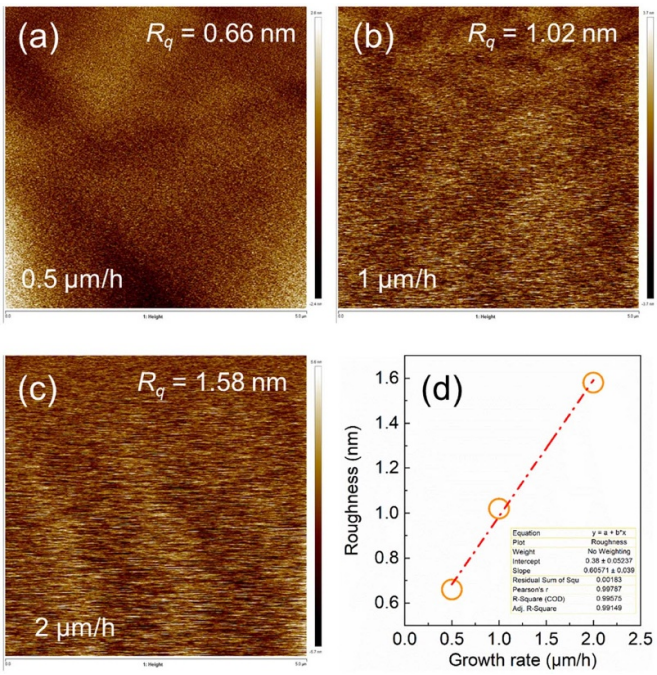

Figure 2. Surface roughness of (a) sample A, (b) sample B, and (c) sample C. (d) Surface roughness as a function of growth rate. The scan area of the AFM image is 5 μm × 5 μm.

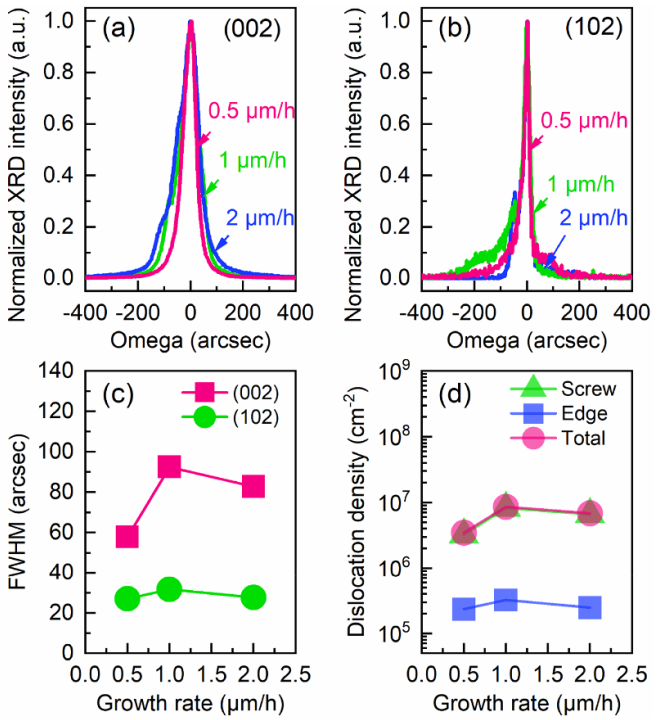

Figure 3. XRDRCs for (a) symmetric (002) and (b) asymmetric (102) reflections. (c) The FWHM for the (002) and (102) planes as a function of growth rate. (d) Screw, edge and total dislocation densities as a function of growth rate.

and (b), respectively. The full-width-half-maximum (FWHM) as a function of growth rate is summarized in figure 3(c). The FWHM for the (002) plane of sample A, sample B, and sample C are 58.0 arcsec, 92.5 arcsec, and 82.8 arcsec, respectively. The FWHM for the (102) plane of the samples is 27.0 arcsec, 31.7 arcsec and 27.7 arcsec, respectively. Based on the FWHM of the two planes, the dislocation density of the samples can be estimated as shown in figure 3(d) [28]. The (002) plane FWHM corresponds to screw dislocations, and the (102) plane FWHM is mainly due to edge dislocations. It can be seen that the edge dislocation density is relatively small and does not change much with increasing growth rate. On the other hand, screw dislocations dominate in the regrown *p*-GaN film. Generally speaking, the screw dislocation density is higher at higher growth rate. The total dislocation densities are estimated to be 3.5×10^6 cm^{-2}, 8.6×10^6 cm^{-2}, and 6.9×10^6 cm^{-2} for sample A, sample B, and sample C, respectively, as shown in figure 3(d).

Transmission electron microscopy (TEM) was used to further investigate the regrown *p–n* junctions as shown in figure 4. Obvious regrowth interfaces can be seen in the TEM images for the samples. According to our previous results, the sharp contrast near the regrowth interface is due to very high concentrations of Si and Mg at the regrowth interface. There are two reasons for the enrichment of the two impurities at the regrowth interface: the regrowth process and Mg/Si co-doping [29]. It should be noted that there is a substantial amount of Mg precipitate in the regrown *p*-GaN of sample A. The appearance of Mg precipitate indicates that the Mg concentration in the regrown *p*-GaN with a low growth rate has exceeded Mg solubility limit in the *p*-GaN, i.e. the *p*-GaN was over-doped [30].

However, no identifiable Mg precipitate was found in the other two samples which have the same Cp_2Mg flow rate but higher growth rates. These results suggest that the growth rate can affect the Mg doping concentration. This makes sense because higher growth rate means larger GaN volume competing for the same amount of Mg, which is equivalent to a decrease in Mg concentration with the same Cp_2Mg flow rate. Higher Mg precipitate could increase the tunneling effect when the *p–n* diode is under reverse bias due to the increased defect density. The p^+–n^+ junction at the regrowth interface due to the high Mg and Si concentrations can make the regrown *p–n* diode behave like a Zener diode that the reverse current density was almost temperature independent [19].

Figure 5(a) shows the Mg concentrations of the samples as a function of growth rate measured by secondary ion mass spectrometry. It is consistent with the TEM results that higher growth rate leads to lower Mg doping concentration. The regrown *p*-GaN layer of sample A with obvious Mg precipitate has the highest Mg doping concentration of 7.0×10^{19} cm^{-3}. The dependence of Mg doping concentration on the growth rate will be a big challenge for selective-area doping using the regrowth approach. The growth rate with a growth mask (e.g. SiO_2) is much higher than that without the mask. This will cause low Mg doping concentration and low conductive *p*-GaN layer, which is detrimental to some GaN devices such as *p*-GaN gated transistors. The regrowth in a patterned region will also lead to non-uniform Mg doping due to the different growth rates on different crystal planes [31, 32].

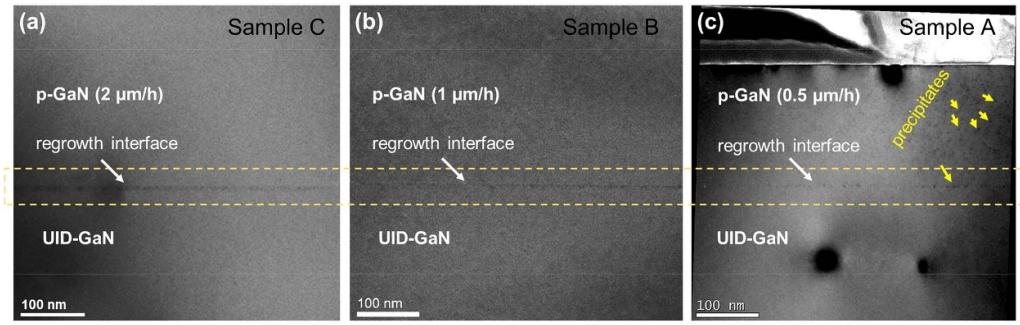

Figure 4. Cross-sectional TEM images of the regrown *p*–*n* junctions with different growth rates.

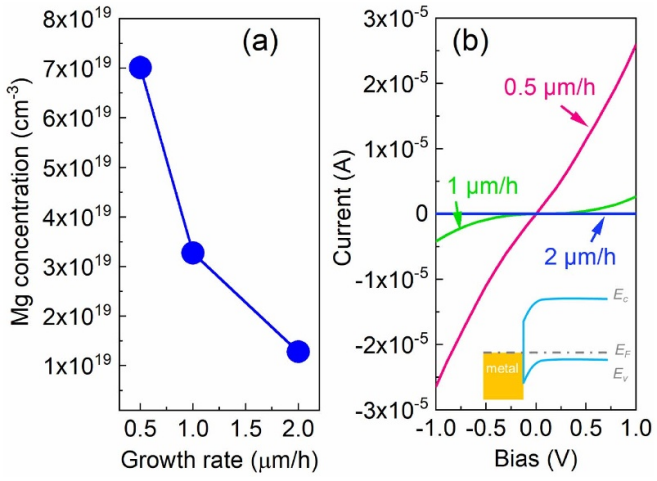

Figure 5. (a) Mg concentration vs growth rate. (b) Current–voltage curves between the ohmic contacts on the regrown *p*-GaN layers of the samples.

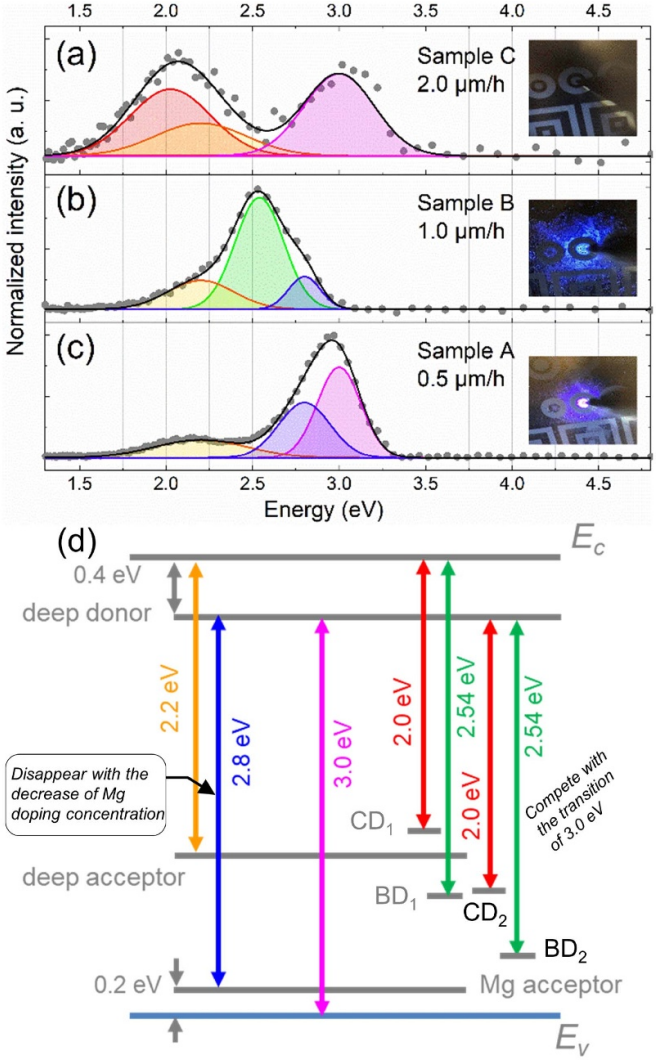

Figure 6. Normalized electroluminescence and fitting spectra using Gaussian equations for (a) sample C, (b) sample B, and (c) sample A. (d) Schematic of possible transitions for the electroluminescence of the samples.

Figure 5(b) shows current–voltage (*I*–*V*) curves between two ohmic contacts using a transmission line method for the samples. Pd/Ni/Au (10 nm/20 nm/50 nm) metal stacks were deposited on the samples by electron-beam evaporation for *p*-GaN ohmic contacts, followed by annealing at 400 °C for 5 min in N_2 ambient. It is obvious that the regrown *p*-GaN layer is more resistive with lower Mg doping concentration caused by higher growth rate.

Figures 6(a)–(c) show normalized EL spectra for the three samples. As shown in the insets, the EL intensity decreased with increasing growth rate due to the decrease in Mg doping concentration. Gaussian equations were used to fit the spectra for further analysis on emission properties. Figure 6(d) presents possible transitions between energy levels in *p*-GaN to explain the EL spectra of the samples. Three EL peaks of 2.2 eV, 2.8 eV, and 3.0 eV were found for sample A. The 2.2 eV peak is related to the capture of conduction band electrons by a deep acceptor level centered at 2.2 eV below the conduction band edge (CBE) [33]. The 2.8 eV peak stems from donor–acceptor pair luminescence due to transition from deep donor level (~0.4 eV below the CBE) to the Mg acceptor level which is ~0.2 eV above valence band edge (VBE) [34, 35]. The 3.0 eV peak is due to the transition from the deep donor to the VBE. Compared with sample A, an obvious change in the spectra of sample B to sample C is the weakening and disappearance of the transition (2.8 eV) from the deep donor level to the Mg acceptor level as the growth rate increases

(or the Mg doping concentration decreases). This phenomenon is due to the reduction of Mg acceptors with the decrease of the Mg doping concentration. For sample B, the transition (3.0 eV) from the deep donor level to the VBE almost disappears, and a new transition peak (2.54 eV) is observed. There are two possible defect-related levels that are responsible for the new transition peak as shown in figure 6(d), which are named BD_1 and BD_2. The disappearance of the transition of 3.0 eV suggests a new competitive process from the deep donor level. Therefore, the trap level BD_2 centered at 0.46 eV above the VBE is the most likely one for the transition in sample B. For sample C, there are also two possible defect-related levels that are responsible for the new transition peak (2.0 eV) shown in figure 6(d), which are named CD_1 and CD_2. The relative reduction in the EL peak of 3.0 eV (figure 6(a)) also indicates the existence of a competitive process compared to the sample A (figure 6(c)). So, the trap level CD_2 centered at 1.0 eV above the VBE is the most likely one for the transition in sample C. The increased screw dislocation density in sample B and sample C is likely to be the cause of these defect levels.

4. Conclusion

In summary, the effects of growth rate on *p*-GaN layers regrown on etched surfaces on free-standing GaN substrates by MOCVD have been comprehensively investigated. The roughness of the samples increases almost linearly with the growth rate at ~0.6 nm ($\mu m\ h^{-1}$) $^{-1}$. The screw dislocation density of the samples increases significantly when the growth rate is higher than 0.5 $\mu m\ h^{-1}$. In addition, under the same Cp_2Mg flow rate, the Mg doping concentration decreases with the growth rate. Obvious regrowth interfaces can be seen in the TEM images of the samples. Mg precipitate was observed in regrown *p*-GaN when the Mg doping concentration was higher than 7.0×10^{19} cm^{-3}. This is because Mg solubility limit has been exceeded and the *p*-GaN was over doped. Furthermore, the samples with different growth rate also show different EL spectra. The transition (2.8 eV) from the deep donor level to the Mg acceptor level diminishes as the growth rate increases (or the Mg doping concentration decreases). Transitions related to defect levels appears with the increase of growth rate due to the increased screw dislocation density at higher growth rates.

Acknowledgments

This work was supported in part by ARPA-E PNDIODES Program monitored by Dr Isik Kizilyalli under Grant No. DE-AR0000868, in part by the NASA HOTTech Program under Grant No. 80NSSC17K0768, and in part by the ASU Nanofab through NSF under Contract ECCS-1542160. We acknowledge the use of facilities within the Eyring Materials Center at Arizona State University. The device fabrication was performed at the Center for Solid State Electronics Research at Arizona State University.

ORCID iD

Kai Fu https://orcid.org/0000-0002-9405-7512

References

[1] Mishra U K, Shen L, Kazior T E and Wu Y 2008 GaN-based RF power devices and amplifiers *Proc. IEEE* **96** 287–305
[2] Baliga B J 2013 Gallium nitride devices for power electronic applications *Semicond. Sci. Technol.* **28** 074011
[3] Ueda T 2019 GaN power devices: current status and future challenges *Japan. J. Appl. Phys.* **58** SC0804
[4] Kucheyev S, Williams J and Pearton S 2001 Ion implantation into GaN *Mater. Sci. Eng.* R **33** 57
[5] Sheu J K and Chi G C 2002 The doping process and dopant characteristics of GaN *J. Phys.: Condens. Matter.* **14** R657
[6] Zhang A P, Han J, Ren F, Waldrip K E, Abernathy C R, Luo B, Dang G, Johnson J W, Lee K P and Pearton S J 2001 GaN bipolar junction transistors with regrown emitters *Electrochem. Solid State* **4** G39–G41
[7] Hong S J, Chapman P, Krein P T and Kim K 2006 Selective-area growth and fabrication of recessed-gate GaN MESFET using plasma-assisted molecular beam epitaxy *Phys. Status Solidi* A **203** 1872–5
[8] Wen Y *et al* 2011 Enhancement-mode AlGaN/GaN heterostructure field effect transistors fabricated by selective area growth technique *Appl. Phys. Lett.* **98** 072108
[9] Yang F *et al* 2015 The suppression of background doping in selective area growth technique for high performance normally-off AlGaN/GaN MOSFET *J. Mater. Sci., Mater. Electron.* **26** 9753–8
[10] Pang L, Seo H-C, Chapman P, Adesida I and Kim K 2010 Breakdown voltage enhancement of AlGaN/GaN high-electron-mobility transistors via selective-area growth for ohmic contacts over ion implantation *J. Electron. Mater.* **39** 499–503
[11] Singisetti U, M H W, Dasgupta S, Nidhi , Swenson B, Thibeault B J, Speck J S and Mishra U K 2011 Enhancement-mode N-polar GaN MISFETs with self-aligned source/drain regrowth *IEEE Electron Device Lett.* **32** 137–9
[12] Guo J *et al* 2012 MBE-regrown ohmics in InAlN HEMTs with a regrowth interface resistance of 0.05 Ω·mm *IEEE Electron Device Lett.* **33** 525–7
[13] Yue Y *et al* 2012 InAlN/AlN/GaN HEMTs with regrown ohmic contacts and f_T of 370 GHz *IEEE Electron Device Lett.* **33** 988–90
[14] Chowdhury S, Wong M H, Swenson B L and Mishra U K 2012 CAVET on bulk GaN substrates achieved with MBE-regrown AlGaN/GaN layers to suppress dispersion *IEEE Electron Device Lett.* **33** 41–43
[15] Shibata D, Kajitani R, Ogawa M, Tanaka K, Tamura S, Hatsuda T, Ishida M and Ueda T 2016 1.7 kV/1.0 mΩcm2 normally-off vertical GaN transistor on GaN substrate with regrown *p*-GaN/AlGaN/GaN semipolar gate structure *2016 IEEE Int. Electron Devices Meeting (IEDM)* pp 10.1.1–4
[16] Fu K, Fu H, Huang X, Yang T, Chen H, Baranowski I, Montes J, Yang C, Zhou J and Zhao Y 2019 Threshold switching and memory behaviors of epitaxially regrown GaN-on-GaN vertical *p–n* diodes with high temperature stability *IEEE Electron Device Lett.* **40** 375–8
[17] Hu Z, Nomoto K, Qi M, Li W, Zhu M, Gao X, Jena D and Xing H G 2017 1.1-kV vertical GaN *p–n* diodes with *p*-GaN regrown by molecular beam epitaxy *IEEE Electron Device Lett.* **38** 1071–4
[18] Fu K, Fu H, Huang X, Chen H, Yang T, Montes J, Yang C, Zhou J and Zhao Y 2019 Demonstration of 1.27 kV etch-then-regrow GaN *p–n* junctions with low leakage for

GaN power electronics *IEEE Electron Device Lett.* **40** 1728–31
[19] Fu K *et al* 2018 Investigation of GaN-on-GaN vertical *p–n* diode with regrown *p*-GaN by metalorganic chemical vapor deposition *Appl. Phys. Lett.* **113** 233502
[20] Xing H, DenBaars S P and Mishra U K 2005 Characterization of AlGaN/GaN*p–n* diodes with selectively regrown n-AlGaN by metal-organic chemical-vapor deposition and its application to GaN-based bipolar transistors *J. Appl. Phys.* **97** 113703
[21] Koblmüller G, Chu R M, Raman A, Mishra U K and Speck J S 2010 High-temperature molecular beam epitaxial growth of AlGaN/GaN on GaN templates with reduced interface impurity levels *J. Appl. Phys.* **107** 043527
[22] Azize M, Bougrioua Z and Gibart P 2007 Inhibition of interface pollution in AlGaN/GaN HEMT structures regrown on semi-insulating GaN templates *J. Cryst. Growth* **299** 103–8
[23] Cordier Y, Azize M, Baron N, Chenot S, Tottereau O and Massies J 2007 AlGaN/GaN HEMTs regrown by MBE on epi-ready semi-insulating GaN-on-sapphire with inhibited interface contamination *J. Cryst. Growth* **309** 1–7
[24] Fu K *et al* 2020 Reverse leakage analysis for as-grown and regrown vertical GaN-on-GaN Schottky barrier diodes *IEEE J. Electron Devices Soc.* **8** 74–83
[25] Tahhan M, Nedy J, Chan S H, Lund C, Li H, Gupta G, Keller S and Mishra U 2016 Optimization of a chlorine-based deep vertical etch of GaN demonstrating low damage and low roughness *J. Vac. Sci. Technol.* A **34** 031303
[26] Kao -C-C, Huang H W, Tsai J Y, Yu C C, Lin C F, Kuo H C and Wang S C 2004 Study of dry etching for GaN and InGaN-based laser structure using inductively coupled plasma reactive ion etching *Mater. Sci. Eng.* B **107** 283–8
[27] Zhang T *et al* 2019 A >3 kV/2.94 m Ω·cm2 and low leakage current with low turn-on voltage lateral GaN Schottky barrier diode on silicon substrate with anode engineering technique *IEEE Electron Device Lett.* **40** 1583–6
[28] Fu H, Huang X, Chen H, Lu Z, Zhang X and Zhao Y 2017 Effect of buffer layer design on vertical GaN-on-GaN *p–n* and Schottky power diodes *IEEE Electron Device Lett.* **38** 763–6
[29] Alugubelli S R, Fu H, Fu K, Liu H, Zhao Y, McCartney M R and Ponce F A 2019 Determination of electronic band structure by electron holography of etched-and-regrown interfaces in GaN *p-i-n* diodes *Appl. Phys. Lett.* **115** 201602
[30] Hansen M, Chen L F, Lim S H, DenBaars S P and Speck J S 2002 Mg-rich precipitates in the *p*-type doping of InGaN-based laser diodes *Appl. Phys. Lett.* **80** 2469–71
[31] Liu H, Fu H, Fu K, Alugubelli S R, Su P-Y, Zhao Y and Ponce F A 2019 Non-uniform Mg distribution in GaN epilayers grown on mesa structures for applications in GaN power electronics *Appl. Phys. Lett.* **114** 082102
[32] Yang C *et al* 2020 GaN vertical-channel junction field-effect transistors with regrown *p*-GaN by MOCVD *IEEE Trans. Electron Devices* **67** 3972–7
[33] Shalish I, Kronik L, Segal G, Rosenwaks Y, Shapira Y, Tisch U and Salzman J 1999 Yellow luminescence and related deep levels in unintentionally doped GaN films *Phys. Rev.* B **59** 9748–51
[34] Kaufmann U, Kunzer M, Maier M, Obloh H, Ramakrishnan A, Santic B and Schlotter P 1998 Nature of the 2.8 eV photoluminescence band in Mg doped GaN *Appl. Phys. Lett.* **72** 1326–8
[35] Reshchikov M A, Yi G C and Wessels B W 1999 Behavior of 2.8- and 3.2-eV photoluminescence bands in Mg-doped GaN at different temperatures and excitation densities *Phys. Rev.* B **59** 13176–83